SAE International Journal of Materials and Manufacturing

Influence of strain rate effect on mechanical and crashworthiness properties of CFRP composite structures

Abstract:

Composite materials are increasingly utilised in industries such as automotive and aerospace due to their lightweight nature and high strength-to-weight ratio. Understanding how strain rate affects the mechanical and crashworthiness properties of CFRP composites is essential for accurate impact simulations and improved safety performance. This study examines the strain rate sensitivity of CFRP composites through mechanical testing and finite element analysis (FEA). Experimental results confirm that compressive strength increases by 100–200% under dynamic loading, while stiffness decreases by up to 22% at a strain rate of 50 s^{-1}, consistent with trends observed in previous studies. A sled test simulation using LS-Dyna demonstrated that the CFRP crash box sustained an average strain rate of 46.5 s^{-1}, aligning with realistic impact conditions. Incorporating strain rate-dependent material properties into the FEA model significantly improved correlation with experimental crashworthiness data, reducing discrepancies in peak acceleration, mean acceleration, and displacement by 6.5%, 5.9%, and 6.3%, respectively. These findings reinforce the necessity of accounting for strain rate effects in crash simulations and composite structure design, ensuring more accurate predictions of impact performance and structural integrity in safety-critical applications.

Keywords: Composites; crash box; crashworthiness; lightweight; Strain-rate; mechanical testing; dynamic test

1. Introduction

In recent years, Composite materials have increasingly replaced traditional metals like aluminium and steel in various industries such as aerospace, automotive, defence, and energy due to their superior mechanical properties, lightweight nature, corrosion resistance, and electrical insulation [1,2]. In the automotive sector, composites offer a cost-effective solution, enabling the development of lighter, more economical vehicles with fewer components while enhancing design flexibility [1].

One of the key applications of composites in vehicle safety is in energy absorbers, initially introduced as metallic crash boxes to absorb impact energy. Traditionally made from steel, these crash boxes are now being replaced with aluminium and fibre-reinforced composite polymers [1,3]. As vehicle performance advances, stricter safety regulations require a detailed assessment of structural crashworthiness. While metallic crash boxes dissipate impact energy through progressive deformation mechanisms such as bending, buckling, and folding, composite crash boxes rely on fracture-based energy absorption mechanisms, including fibre breakage, matrix cracking, delamination, and fibre-matrix debonding [1,3]. The effectiveness of a composite crash box depends on several factors, including fibre type, matrix properties, volume fraction, fibre orientation, stacking sequence, and structural geometry [3].

To evaluate crashworthiness, composite crash structures undergo drop tests, where components experience controlled impact conditions. Since impact tests involve dynamic loading, it is crucial to understand how the mechanical properties of composites change at different strain rates [2,4].

Over the past decade, research into the strain rate dependency of composite laminates has grown significantly. Early studies suggested minimal strain rate effects in unidirectional composites loaded in

the fibre direction due to the dominance of fibre properties [7,8]. However, later studies demonstrated that strain rate significantly influences mechanical properties, particularly in off-axis and cross-ply laminates. Amos, Robert, and Gary [9] investigated the tensile strain-rate behaviour of IM7/997-2 carbon/epoxy laminates, reporting an increase in both strength and stiffness, with a more pronounced dependency for 45° and ±45° fibre orientations. Since stiffness depends on both material properties and structural geometry, an increase in Young's modulus under dynamic loading enhances the structural stiffness of composite crash components. This effect is particularly relevant in fibre-reinforced composites, where strain rate sensitivity improves load-bearing performance. Montiel and Williams [10] studied the dynamic behaviour of cross-ply AS4 graphite-PEEK laminates at a strain rate of 8 s^{-1} using a drop tower test, finding a 42% increase in strength and a 25% increase in failure strain [10,11].

Similarly, researchers at the University of Delaware examined the dynamic response of composite laminates at strain rates up to 1200 s^{-1}, demonstrating a strong dependency between strain rate and mechanical properties [12]. While many studies have explored strain rate effects at the material level, fewer have examined their influence on full-scale composite crash structures. This gap highlights the need for dynamic testing at the component level to improve crashworthiness predictions.

While quasi-static crash test results show good agreement across different studies, dynamic crash test data often exhibit variability [2]. Redouane et al. [13] performed experimental and numerical analyses on composite energy absorbers and found that low-velocity dynamic crash tests (4.6 m/s) had lower energy absorption capacity than quasi-static tests but exhibited higher peak crash forces. Similarly, Matthew and Alaster [14] validated these findings through FEA-based impact simulations, demonstrating that dynamic material properties improve numerical-experimental correlation, with higher initial peak forces and lower average crash forces compared to quasi-static models.

Although many studies have explored the use of composites in crash structures, this study extends the investigation to the component level by evaluating strain rate effects on the crashworthiness of CFRP crash boxes in electric vehicle applications. By incorporating experimental testing and numerical validation, this study bridges the gap between material-level investigations and real-world crashworthiness assessments, providing a more comprehensive understanding of strain rate effects on CFRP crash structures. The research integrates mechanical testing, finite element simulations, and sled impact testing, bridging the gap between material-level studies and full-scale crash performance assessments.

2. Strain rate effect on CFRP mechanical properties

Two types of mechanical tests were performed to acquire the material properties needed for the development of the material card based on which the crash simulations were performed. Tensile and compression testing were conducted under quasi-static and dynamic conditions to study the change in properties with respect to strain rate. to each coupon a 2-axis strain gauge was attached to provide the information with respect to 2 directions in-line with the CFPR lay-up used in this paper. Usage of the strain-gauges allowed us to have more accurate characterisation of material properties.

2.1 Tensile test

The quasi-static and dynamic tensile tests were conducted in accordance with the ASTM D3039 standard for the quasi-static test and BS EN ISO 527-5 for the dynamic test [17,18]. The material properties of interest included the maximum strength and strain, Young's modulus, Poisson's ratio and

strain rates. These were obtained from the preparation and testing of five specimens for each case under study at nominal dimensions of 250mm length, 25mm width, and 2.4mm thickness for the quasi-static case. For the dynamic tests a dogbone shape of 400mm length, 25mm width in the gauge area, and 2.4mm thickness was used.

Biaxial strain gauges were attached on both sides of each specimen for the measurement of the strain, Time, force and displacement during the testing until the ultimate failure of the specimens. The values recorded during testing were transformed into stress-strain curves for the extraction of the material properties in the fibre direction. The tensile young's modulus was calculated over a strain range from 0.0005 to 0.0025 absolute strain, with corresponding tensile stress values corresponding to these strain points. EQ1 describes the calculation of Young's modulus.

$$E^t = \frac{\Delta\sigma_{11}}{\Delta\varepsilon_{11}} \qquad \boldsymbol{EQ\ 1}$$

Here, Δε is the strain range difference between 0.0005 and 0.0025 absolute strain and Δσ is the difference of stress values corresponding to these strains. The subscript *t* corresponds to tensile, whilst *22* and *11* are used to represent the transverse and longitudinal directions, respectively. The Poisson's ratio *v* was determined with respect to the strains in the longitudinal and transverse directions. The longitudinal strain range corresponds to the strain range from 0.0005 to 0.0025 absolute strain, and their corresponding transverse strain values were determined through plotting. Both the Poisson's ratio and the strain rate"$\dot{\varepsilon}$" are calculated in EQ2 and EQ3, respectively.

$$v^t = -\frac{\Delta\varepsilon_{22}}{\Delta\varepsilon_{11}} \qquad \boldsymbol{EQ\ 2}$$

$$\dot{\varepsilon} = \frac{d\varepsilon}{dt} \qquad \boldsymbol{EQ\ 3}$$

2.1.1 Quasi-static test

The quasi-static tests were performed using an Instron 8801 B909 servo-hydraulic test machine with a head cross displacement of 2mm/min. The tests were performed on cross-ply laminates for carbon fibre specimens at loading directions of 0° and 90° at room temperature.

2.1.2 Dynamic test

The dynamic tests were performed using a high strain rate VHS Instron test machine at velocities of 5, 10 and 15.5m/s resulting to average strain rates values of 30, 65 and 128s^{-1} respectively. The tests were performed on cross-ply laminates for carbon fibre specimens at loading directions of 0° and 90° at room temperature.

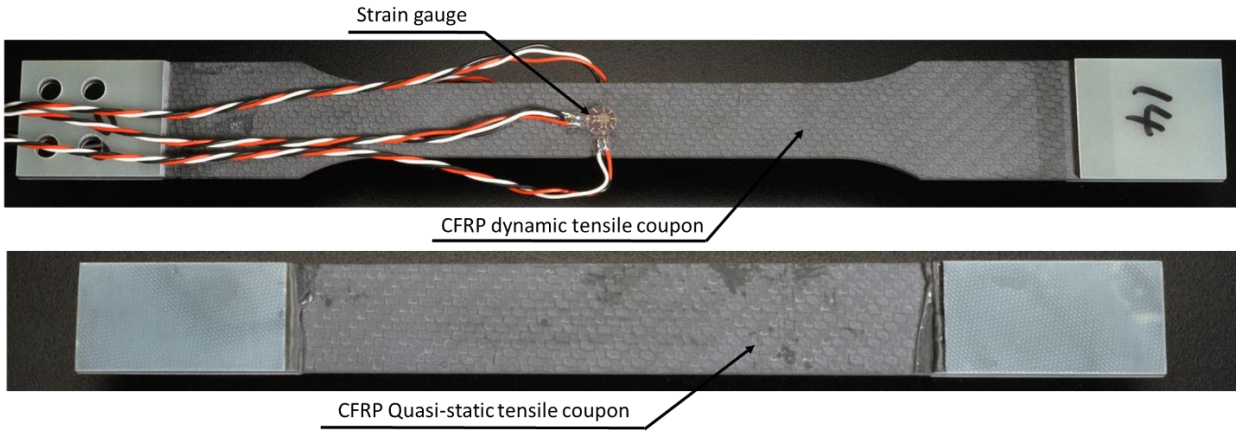

Figure 1 - quasi-static and dynamic tensile coupon configuration

2.2 Compression test

Quasi-static and dynamic compression tests took place in accordance with ASTM D6641 standard [19]. The acquired material properties included maximum strength and strain, modulus, Poisson's ratio, and strain rates. These were obtained from the preparation and testing of five specimens for each case under study at nominal dimensions of 140mm length, 13mm width, and 2.4mm thickness.

The strain measurement was carried out through biaxial strain gauges attached on both sides of each specimen. Time, force, displacement, and strain were recorded during the testing until the ultimate failure of the specimens. The compressive modulus was calculated within the strain range of 0.001 to 0.003 absolute strain and the respective compressive stress values corresponding to these strain points. The equation describing the calculation of the compressive modulus is the shown in EQ4.

$$E^c = \frac{\Delta\sigma_{11}}{\Delta\varepsilon_{11}} \qquad \boldsymbol{EQ\ 4}$$

Here, Δε is the strain range difference between 0.001 and 0.003 absolute strain and Δσ is the difference in stress values corresponding to them. Subscript "c" *c*orresponds to compression, whilst *22* and *11* are used to represent the transverse and longitudinal directions, respectively. The Poisson's ratio *v* was determined with respect to the strains in the longitudinal and transverse directions. The longitudinal strain range corresponds to the strain range at 0.001 and 0.003 absolute strain and their corresponding transverse strain values are determined through plotting. The compressive Poisson's ratio was calculated as illustrated in EQ5.:

$$v^c = -\frac{\Delta\varepsilon_{22}}{\Delta\varepsilon_{11}} \qquad \boldsymbol{EQ\ 5}$$

2.2.1 Quasi-static test

Quasi-static tests were performed using an Instron 8800 B530 servo-hydraulic test machine (Figure 2) with a head cross displacement of 2mm/min). The tests were performed on cross-ply laminates for carbon fibre specimens at loading directions of 0° and 90° at room temperature.

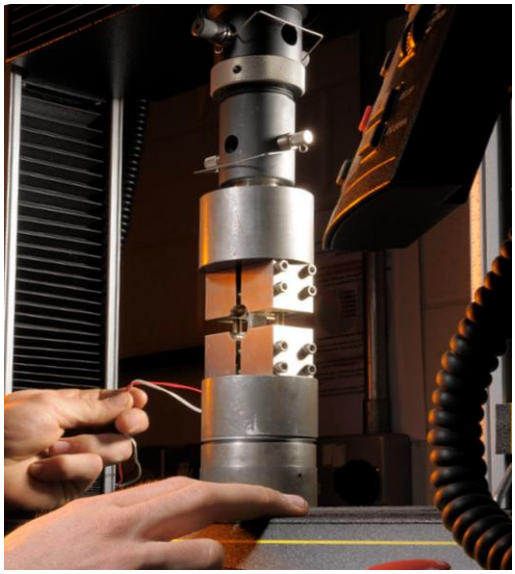

Figure 2 - Compression test configuration

2.2.2 Dynamic

Dynamic compression testing was performed using a high strain rate VHS (Visco-Hyperelastic Strain) Instron test machine at velocities of 5 and 7.5m/s. The tests were carried out on cross-ply laminates for carbon fibre specimens at loading directions of 0° at RT as shown in Figure 3.

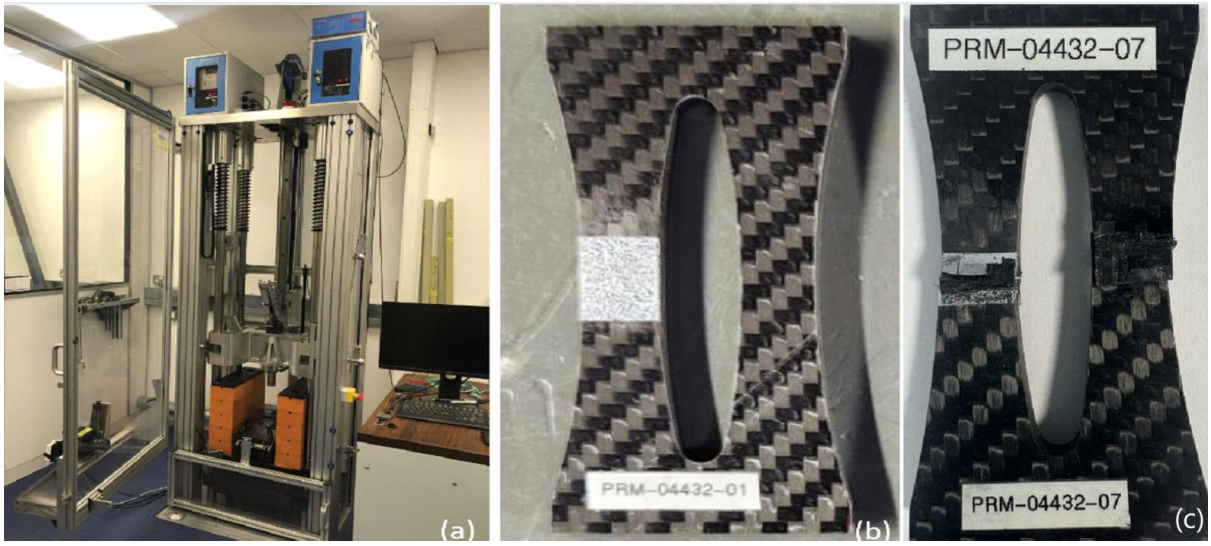

Figure 3 - Dynamic compression test specimen and configuration a) test set-up b) test sample c) broken sample after the test

2.3 Data analysis

The longitudinal and transverse tensile test results are presented in Figure 4 and Figure 5, respectively, identifying the change in maximum stress, strain and modulus ratio (Dynamic/Quasi-static) in relation to the strain rate. As expected, the tensile results in longitudinal direction are higher than the transverse direction due to the composite lay-up configuration. This is because composite materials exhibit greater tensile resistance along the fibre direction, where the load is primarily carried by the reinforcing fibres, resulting in enhanced stiffness and strength. As evident from these figures, on average the maximum strain at failure decreases as the strain rate increases. As for the maximum strength, the longitudinal strength increases with an increase of the strain rate up to $30s^{-1}$ then it

decreases. Additionally, the modulus shows high dependency on strain rate where it increased by 200%.

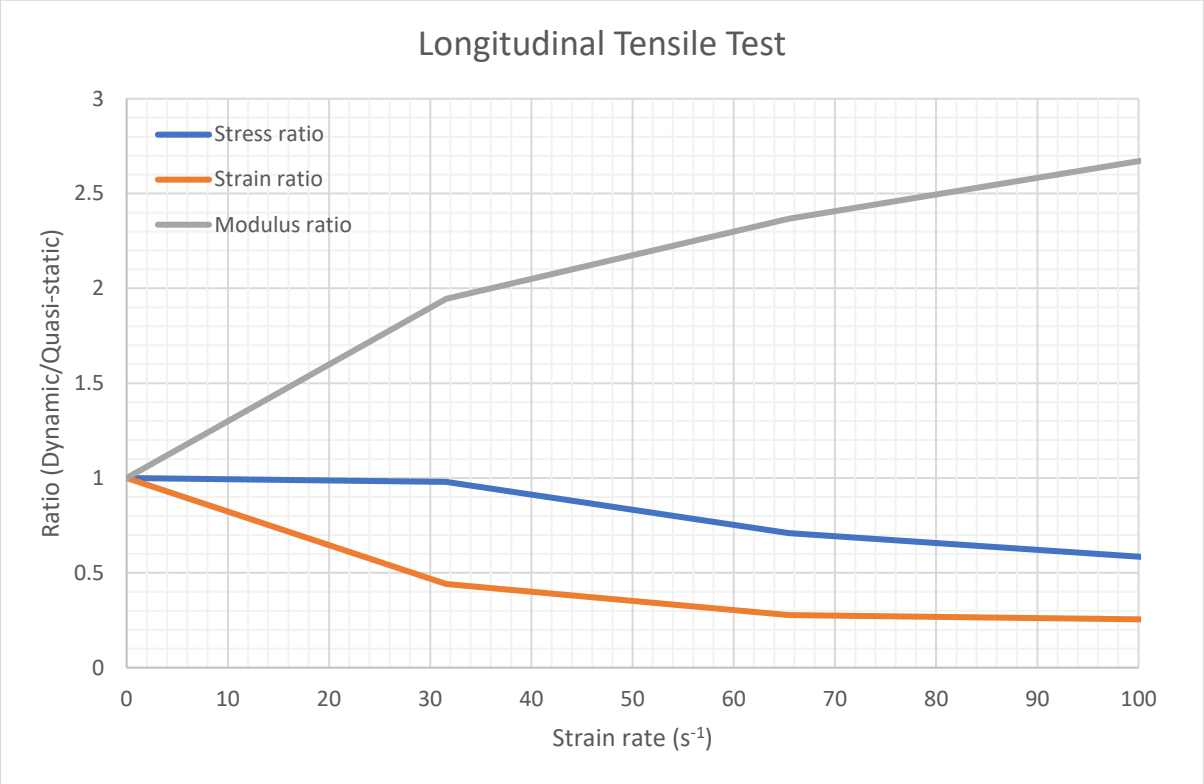

Figure 4 - Longitudinal tensile test results

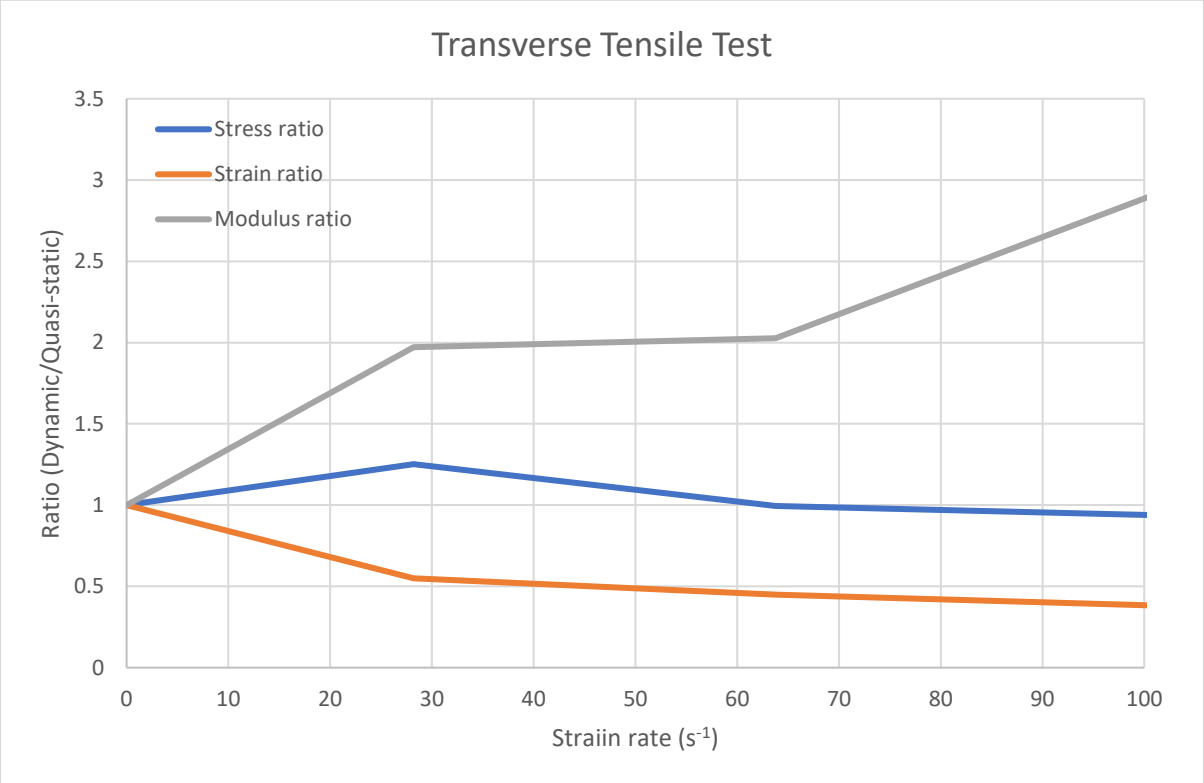

Figure 5 - Transverse tensile Test results

The test results for longitudinal and transverse compression tests are presented in Figure 6 and Figure 7. Both maximum stress and strain at failure increase with the strain rate increase. The compression properties of composite are shown to be most sensitive to the strain rate where the strength was increased by 100% to 200%, however the stiffness of the material decreases by a maximum 22% at a strain rate equal to $50s^{-1}$.

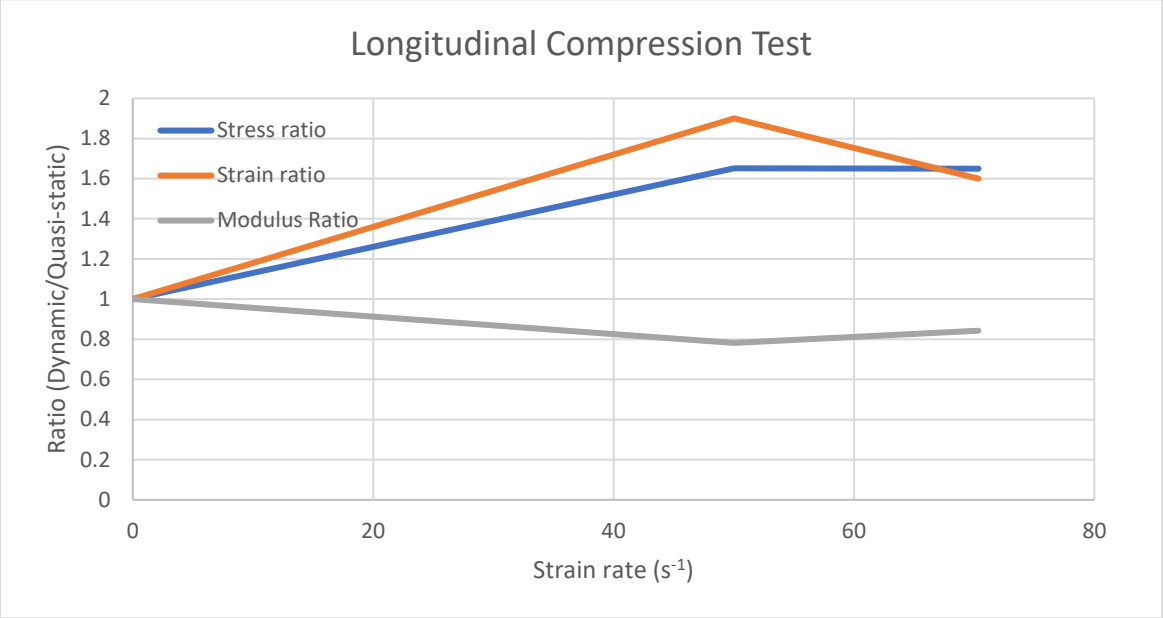

Figure 6 - Longitudinal compression test results

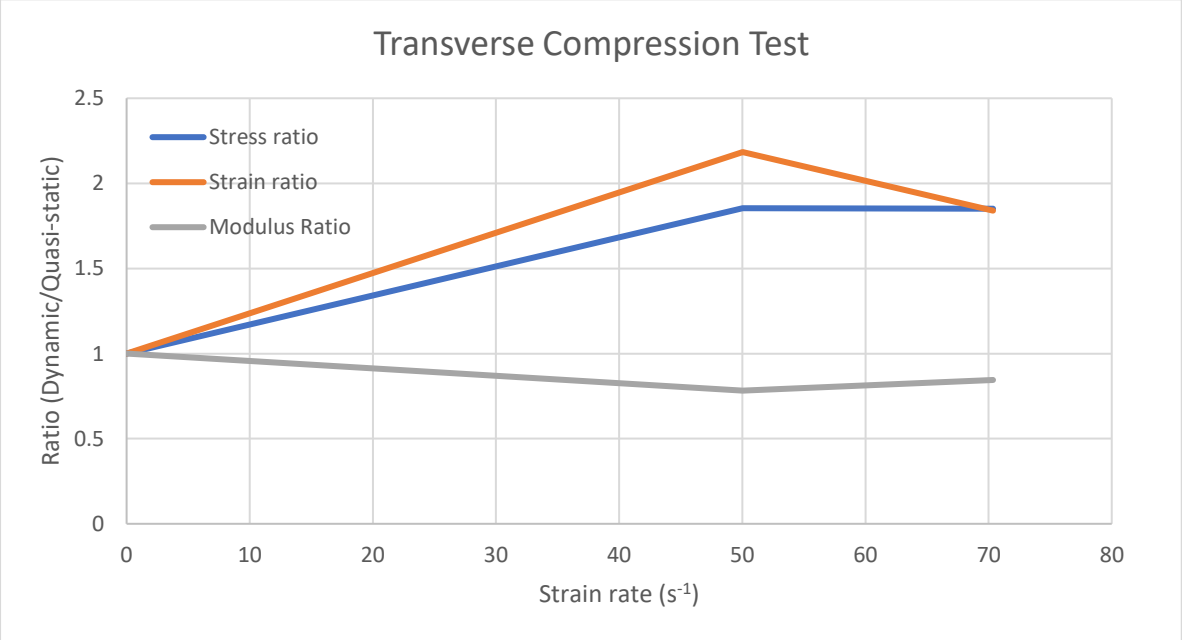

Figure 7 - Transverse compression test results

3. Strain rate effect on CFRP crashworthiness properties

3.1 Introduction to crashworthiness of composites

The crashworthiness capability of an energy absorber is assessed through its ability to absorb energy. The requirement for energy absorbers are to be able to absorb the impact energy with less weight

while maintaining the reaction force (or impact acceleration) low. The composite crash boxes are lightweight, and provide higher energy absorption per unit mass compared to the metallic ones.

Before analysing the impact behaviour of a composite crash box, it is important to identify the variables that defines the crashworthiness behaviour of the structure. These variables are known as the crashworthiness parameters, are outlined as follows:

- Initial Peak Acceleration (force)
- Average Acceleration (force)
- Energy absorbed (EA)
- Stroke length

The Force – Displacement (or Acceleration – Time) curve of an impact test, is an important parameter used to study the crashworthiness behaviour of the structure. The crashworthiness parameters are obtained from this curve.

The initial Peak Acceleration is another significant design requirement for the energy absorbers as it is associated with safety regulations. The average acceleration (force) is another crucial parameter used to study the crashworthiness behaviour of the structure as it identifies the sustained acceleration (or force) by the structure. Based on the design requirements, the initial peak and average acceleration should be kept below an identified threshold.

A typical force–displacement curve for a square tube composite crash box is provided in Figure 8, and it features the initial peak and average force. The structure's energy absorbed (EA) is obtained from the area under the force-displacement curve. The specific energy absorption (SEA) of a structure is EA per unit mass, and it is used to study the capability of a material to absorb energy [3].

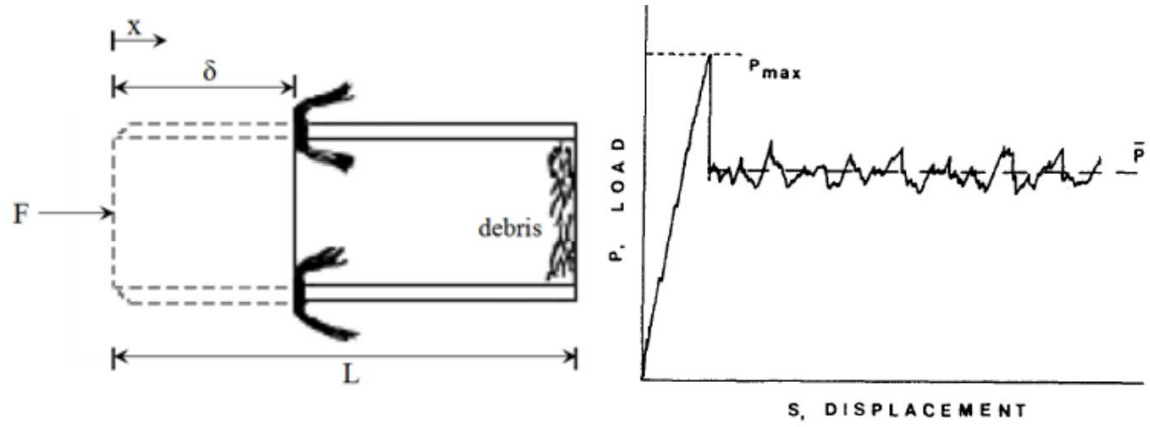

Figure 8 - Force-displacement curve of a square tube composite crash box subjected to axial impact force [15]

3.2 Experimental campaign – sled test

To study the crashworthiness properties of vehicle structures, impact tests were conducted using a sled test. The test evaluates the impact behaviour of the complete crash structure of the vehicle including the crash boxes and the bumper. This test is performed by striking an impactor (rigid body) with initial velocity until the impactor comes to rest (velocity = 0m/s).

The composite crash box was fabricated using vacuum bagging technique also known as vacuum bag laminating fabrication method. This method uses vacuum pressure to apply uniform and constant pressure to the prepreg during their curing.

Figure 9 illustrates the experimental setup for the sled test. In this test, the crash can is mounted on the specimen clamp at the bottom. The impactor weighing of 230Kg and an initial velocity equal to 13.89m/s (50km/h). During the test, the data was captured using an accelerometer.

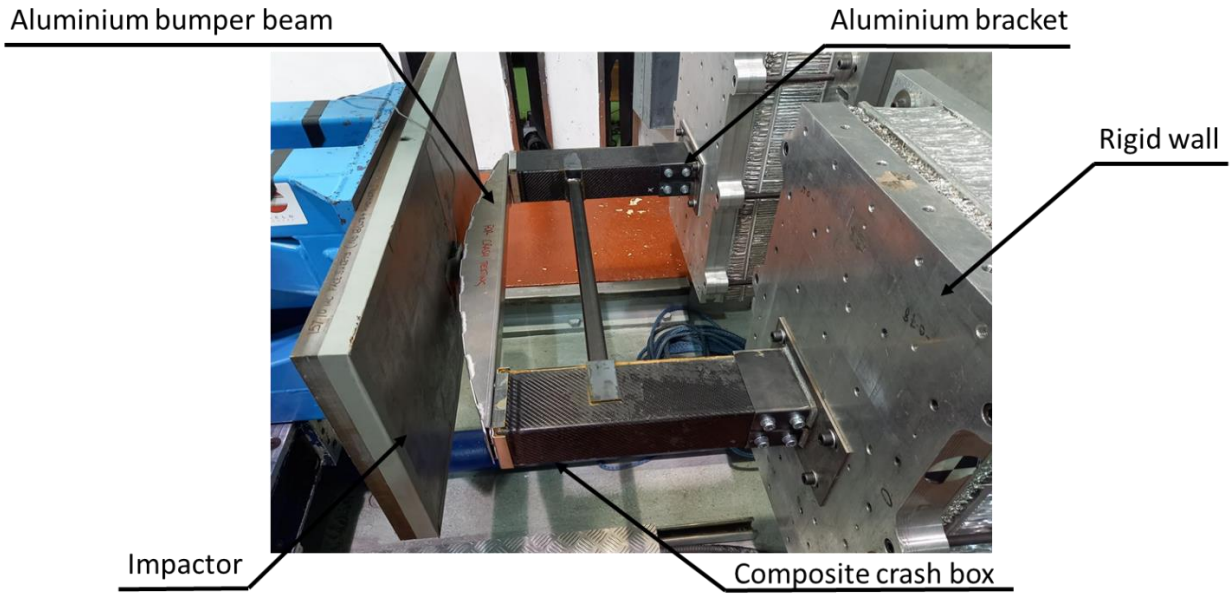

Figure 9 - Sled test configuration

3.3 FEA analysis

To investigate the effect of strain rate on the impact behaviour of the composite crash box, two FEA models with dynamic loading conditions were developed. The first model contained quasi-static material properties while the other had dynamic material properties to consider the strain rate effect on material properties. The impactor had a mass of 830Kg and an initial velocity equal to 13.89 m/s. The Figure 10 shows the flowchart followed for the strain rate dependency analysis.

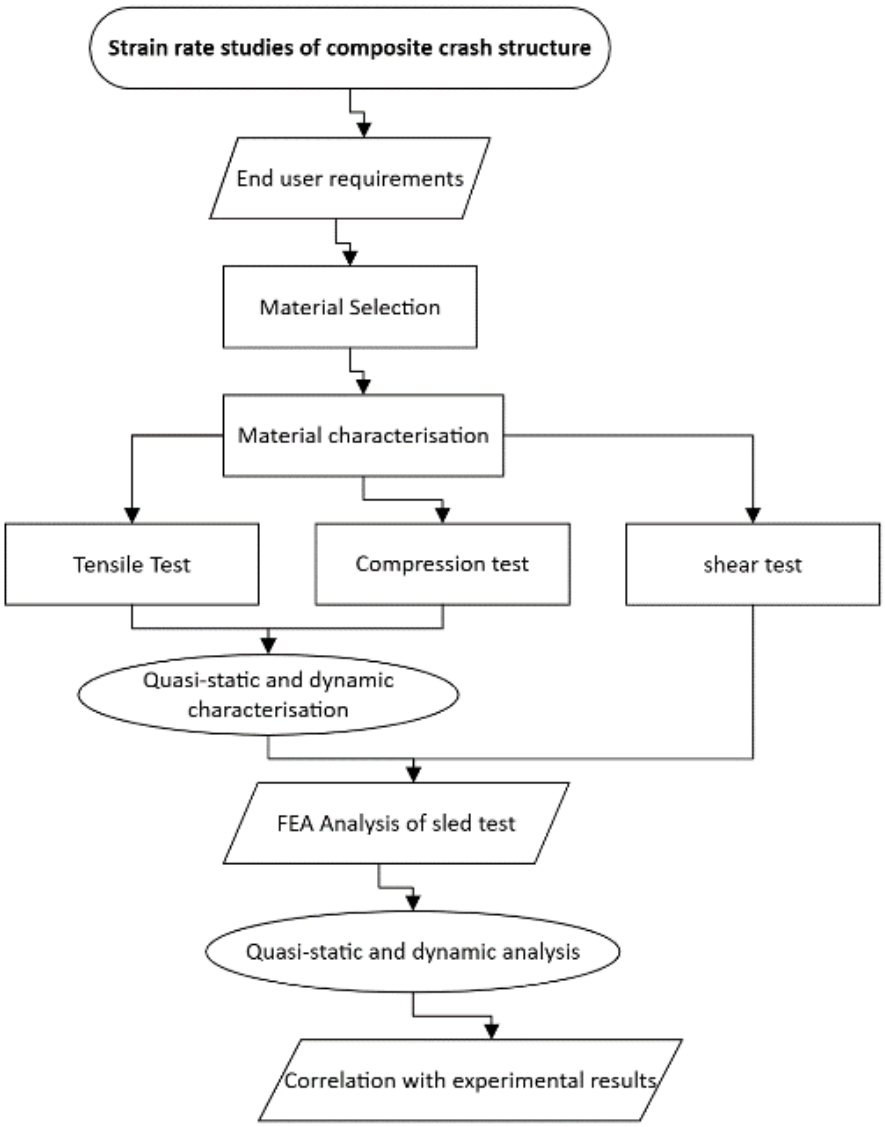

Figure 10 - Flowchart of the strain rate dependency

3.3.1 Modelling approach

The crash box under investigation is a multi-cellular crash box designed with bounded c-sections and an insert bonded with adhesive. It has a length of 420mm and a thickness of 2mm. The adhesive section was designed using MAT_24 (MAT_Piecewise_Linear_Plasticity).

The bounded sections were contacted to the composite c-sections using *tied_shell_to_edge_surface* contact. Additionally, to prevent self-penetration in the model during the impact, an *automatic_single_surface* contact was designed.

The crash structure was secured at the bottom using a rigid wall, and the impactor was modelled as a rigid body with an initial velocity. Additionally, a termination sensor was designed to terminate the model when the impactor's velocity reaches 0m/s. The FEA model is presented in Figure 11 as follows.

The crash box is designed as a multi-wall composite panels joined together using adhesives. The composite parts were joined the adhesive parts using the Tied-Shell_Edge_To_Surface_Beam_Offset.

The Automatic_Surface_To_Surface contact was modelled to connect the crash structure with the rigid wall and the impactor.

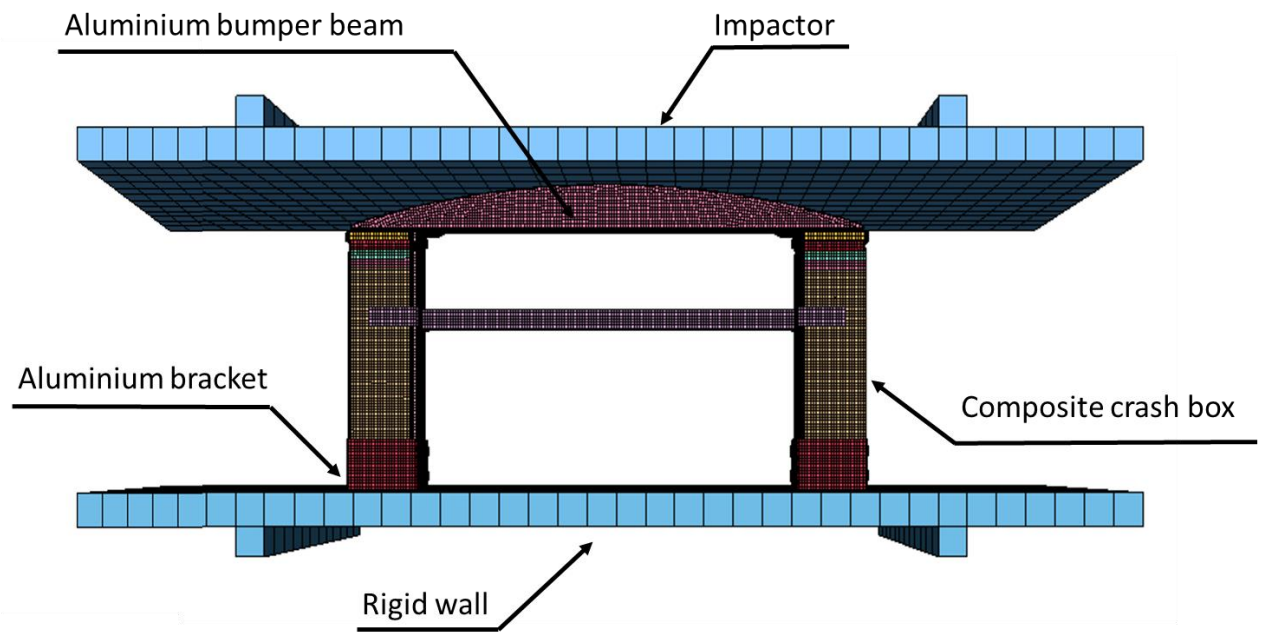

Figure 11 - FEA sled test configuration

3.3.2 Material model

The composite material discussed for this report is a Reinforced carbon fibre composite developed in section 2. To study the crashworthiness properties of the structures, two types of material cards were developed for the composite structures, namely static and dynamic material cards. The dynamic material card was designed by introducing the strain rate to the strength and strain of the material in the static material card.

The dynamic material card involves the realistic response of the structures under the impact. This helps to stabilise the FEA model and have a better correlation between FEA and experimental results. Both dynamic and static material cards were developed using MAT_LAMINATED_COMPOSITE_FABRIC (MAT-58) in LS-Dyna software [16].

MAT-58 is a damage mechanics-based material model available in LS-Dyna that can be implemented into thin shells, thick shells and solid elements. MAT-58 is one of the few composite material cards that allow the user to study the strain rate dependency of the model by defining the maximum stress and strain with respect to strain rate.

3.4 Data analysis

To have a better understanding on effects of strain rate on crashworthiness behaviour of composite crash structure, the effective strain rate versus the simulation time for each composite element within the FEA model was obtained. The average effective strain rate against the simulation time is shown in Figure 12; indicating that the crash structure sustains an average strain rate equal to 46.5 s^{-1}.

Table 1 provides the crashworthiness data for FEA models and experimental samples. A comparison of the results shows that the static FEA model overestimates the peak acceleration and mean acceleration and underestimates the stroke length by 10.2%, 14.3% and 19.7%, respectively.

Introducing dynamic material properties to the FEA model improved the correlation between FEA and experimental crashworthiness parameters by underestimating the peak and mean acceleration and the stroke length by 6.5%, 5.9% and 6.3%, respectively, showing clear improvements.

To examine the sensitivity of the crashworthiness behaviour of the crash box with respect to the strain rate effect on compressive and tensile properties, two dynamic models were designed. Figure 13 shows the change in crash force efficiency (CFE) for static, dynamic compression (strain rate introduced for compressive properties), and dynamic tension (strain rate introduced for tensile properties) models.

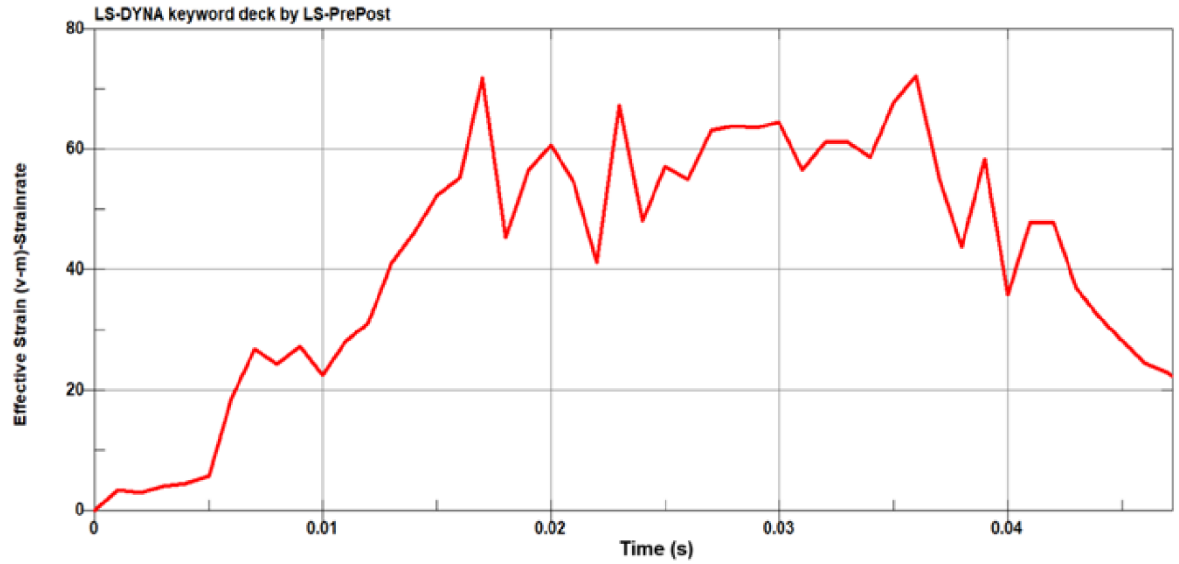

Figure 12 - Average strain rate sustained by the composite crash box

Analysis of the crashworthiness parameters in Figure 13 indicates that the impact behaviour of composite crash box is more sensitive to the compressive material properties than the tensile material properties.

Table 1 - FEA and experimental crashworthiness parameters of the Sled test

	Peak Acceleration (g)	Mean Acceleration (g)	Displacement (mm)
FEA Static	51.9	36.7	277
FEA Dynamic	44.0	30.2	323
EXP - average	47.1	32.1	345

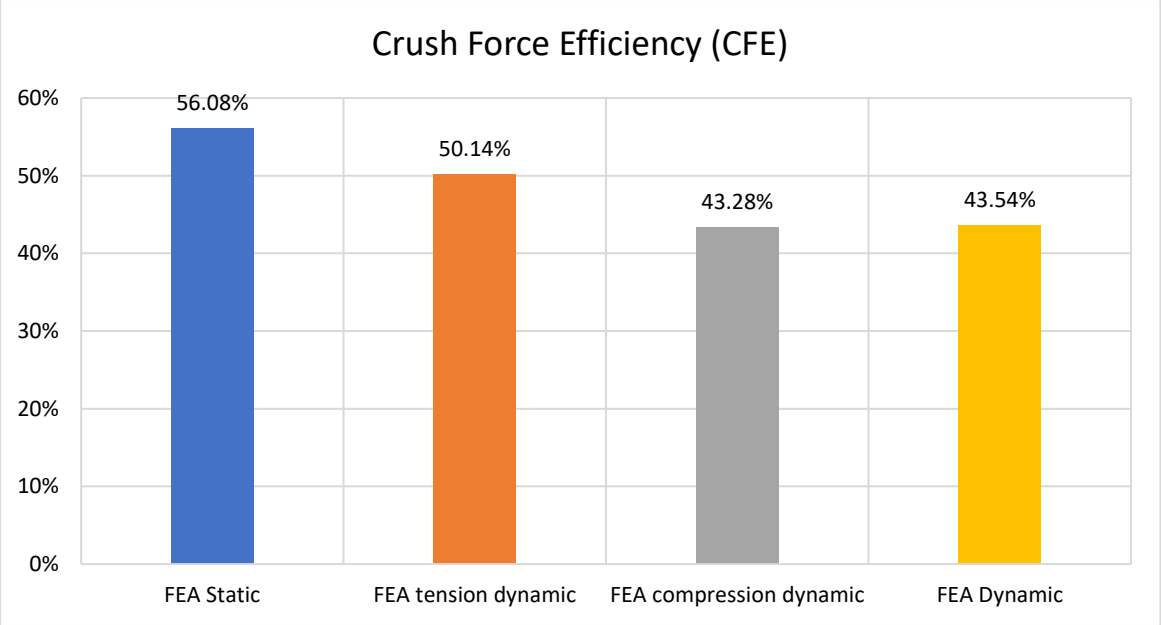

Figure 13 - Crash force efficiency for static and dynamic models

4. Conclusion

This study investigated the strain rate dependency of CFRP composite materials, focusing on their mechanical properties and crashworthiness under axial impact. The findings confirm that composite materials exhibit notable strain rate sensitivity, influencing their mechanical performance and energy absorption characteristics. By integrating quasi-static and dynamic mechanical testing, sled crash experiments, and finite element analysis (FEA), this research provides valuable insights into how strain rate effects influence crashworthiness predictions.

- **Strain Rate Effects on Mechanical Properties**
  - Compressive strength exhibited a clear increase under dynamic loading, demonstrating strain rate sensitivity across the tested range.
  - Stiffness decreased by up to 22% at a strain rate of 50 s^{-1}, highlighting the trade-off between strength and structural flexibility at high strain rates.
  - Higher strain rates resulted in reduced strain at failure, reinforcing the brittle nature of composites under dynamic conditions.

These findings confirm that strain rate influences fundamental mechanical properties, which must be considered in material selection and structural design for impact applications.

- **Crashworthiness Assessment and FEA Validation**
  - Incorporating strain rate-dependent material properties in the FEA model improved correlation with experimental crash test results.
  - The crash box sustained an average strain rate of 46.5 s^{-1} during impact, aligning with real-world crash conditions.
  - The static FEA model overestimated peak acceleration by 10.2% and mean acceleration by 14.3%, while underestimating displacement by 19.7%.

  - The dynamic FEA model reduced these discrepancies to 6.5%, 5.9%, and 6.3%, respectively, demonstrating its superior predictive accuracy.

These results validate the necessity of considering strain rate effects in crash simulations, ensuring better alignment between computational models and real-world crash behaviour.

- **Implications for Composite Crash Structures**
  - Compressive properties were found to be more influential in crash response than tensile properties, emphasizing the need for tailored material properties in crash-prone designs.
  - Incorporating strain rate-dependent properties in simulations significantly enhanced the accuracy of energy absorption and impact force predictions.
  - Accounting for strain rate effects is essential for reliable crashworthiness modelling and structural integrity assessments.

These findings contribute to the optimisation of composite crash structures for automotive and aerospace applications, offering a more robust foundation for designing lightweight, high-performance impact-resistant materials.

Future Work

This research enhances the understanding of strain rate sensitivity in CFRP composites and its role in crashworthiness. By improving FEA predictive accuracy and linking mechanical properties to crash performance, it provides a framework for optimising composite structures in safety critical applications. Future studies should explore a broader range of strain rates, investigate the role of different composite layups and geometries, and refine predictive models to further improve crash simulations.

References

[1] N. Hussain, S. P. Regalla and y. V. Daseswara Rao, “Techniques for correlation of drop weight impact testing and numerical simulation for composite GFRP crash boxes using LS-Dyna,” *International Journal of Crashworthiness,* vol. 27, no. 3, 2022.

[2] X. Liu, B. Belkassem, A. Jonet, D. Lecompte, D. V. Hemelrijck, R. Pintelon and L. Pyl, “Experimental investigation of energy absorptation of circular carbon/epoxy composite tubes under quasi-static and dynamic crush loading,” *Composite Structures,* vol. 27, 2019.

[3] B. Wade and P. Feraboli, “Crushing behaviour of laminated composite structural experiments: Experimental and LS-Dyna simulation,” University of Washington, Washington DC, 2016.

[4] E. R. Tobby and A. Bahaadini, “Design analysis and verification of composite components subjected to crash load cases,” Blekinge Institute of technology, Karlskrona, 2015.

[5] M. A. Courteau, “Investigating the crashworthiness characteristics of carbon fiber/epoxy tubes,” University of Utah, 2011.

[6] R. Foroutan, J. Nemes, H. Ghiasi and P. Hubert, “Experimental Investigation of high strain-rate behaviour of fabric composites,” *Composite Structure,* vol. 106, pp. 264-269, 2013.

[7] J. Harding and L. Welsh, “A tensile testing technique for fibre-reinforced composites at impact rates of strain,” *Journal of Material Science,* vol. 18, pp. 1810-1826, 1983.

[8] T. Schmack, T. Filipe, G. Deinzer, C. Kassapoglou and F. Walther, “Experimental and numerical investigation of the strain rate-dependent compression behaviour of a carbon-epoxy structure,” *Composite Structures,* vol. 189, pp. 256-262, 2018.

[9] A. Gilat, R. K. Goldberg and G. D. Roberts, “Experimental study of strain-rate-dependent behaviour of carbon/epoxy composite,” *Composite Science and Technology,* vol. 62, pp. 1469-1476, 2002.

[10] D. Montiel and C. Williams, “A method for evaluating the high strain compressive properties of composite materials,” *Composite Materials: Testing and design,* vol. 10, 1992.

[11] H. Hsaio and I. M. Daniel, “Strain rate behaviour of composite materials,” *Composite Part B: Engineering,* vol. 29, no. 5, pp. 521-533, 1998.

[12] M. V. Hasur, J. Alexander, U. K. Vaidya and S. Jeelani, “High strain rate compression response of carbon/epoxy laminate composites,” *Composite Structures,* vol. 52, pp. 405-417, 2001.

[13] R. Lombarkia, A. Gakwaya, D. Nandlall, M. L. Dano, J. Levesque, P. Vachon-Joannette, P. Gagnon and A. Benkhelifa, “Strain-rates dependent constitutive law for crashworthiness and parameter sensitivity analysis of wowen composites,” *Aerotecnia Missili & Spazio,* vol. 101, pp. 33-51, 2022.

[14] M. David and A. Johnson, “Effect of strain rate on failure mechanisms and energy absorption in polymer composite elements under axial loading,” *Composite structure,* vol. 122, pp. 430-439, 2015.

[15] D. Hull, “A unified approach to progressive crushing of fibre-reinforced composite tubes,” *Composite Science & Technology,* vol. 40, pp. 377- 421, 1991.

[16] *LSDYNA manuals*. Available at: https://lsdyna.ansys.com/manuals/ (Accessed: 19 August 2024).

[17] ASTM international, ASTMD3039-ASTMD3039M-17, available at: https://cdn.standards.iteh.ai/samples/98550/1ea65d99fa0843b69e4fd81d6a0b55c1/ASTM-D3039-D3039M-17.pdf

[18] i-The standard, ISO 527-5, available at: https://cdn.standards.iteh.ai/samples/80370/6caecb48ef6e4decaabddeebf7ea96ea/ISO-527-5-2021.pdf

[19] ASTM international, ASTMD6641-ASTMD6641M-16, available at: https://cdn.standards.iteh.ai/samples/95932/970e55d110e84fffa29dc7680cc75aa6/ASTM-D6641-D6641M-16.pdf